Electric Field Induced Tunable Electrical Hysteresis in Poly(methyl methacrylate)/ Graphene Oxide Heterostructures

Koustav Kashyap Gogoi[1,a)] and Avijit Chowdhury[1, b)]

[1]*Department of Physics, National Institute of Technology, Silchar-788010, Assam, India*
[a)]koustavgogoitsk@gmail.com
[b)]Corresponding author: avijitiacs@gmail.com

Abstract. Herein, we report the memory properties of multi-stacked graphene oxide (GOs)-PMMA devices sandwiched between ITO and Aluminum as bottom and top electrodes, respectively. GOs was prepared by following the conventional Hummer's method and was analyzed by using the optical and morphological characterization techniques such as Fourier transform infrared spectroscopy (FTIR) and X-ray diffraction (XRD). The current-voltage (I-V) characteristics of the fabricated multi-stacked devices were performed by varying the concentration of GOs. All the devices exhibited electrical hysteresis phenomenon with varying hysteresis area. The hysteresis area was found to increase with increase in the amount of GOs.

INTRODUCTION

Memory properties of polymer based organic memory devices have been drawing a lot of attention in the recent years due to the limitations of conventional silicon based memories [1,2,3]. The exhibition of electrical hysteresis is one of the major features that confirms the presence of memory property in a material [4]. The area under the hysteresis curve and repeatability of such electrical hysteresis under applied bias characterizes the quality of the memory devices. Various materials such as metal oxides [5], transition metal oxides [6], group II-VI semiconductor materials [7,8], graphene oxide [9, 10], carbon nanotubes [11,12] etc., have been found to exhibit memory characteristics when mixed with polymers to from nanocomposites. But the major drawback in the preparation of nanocomposites is the selection of a single solvent which should be capable of dissolving both the active material and the polymer. This limitation can be overcome by multi-stacking the layers of polymer and the nanomaterial. Such kind of fabrication technique does not require a common solvent for the polymer and the nanomaterial thereby simplifying the overall fabrication procedure. At present, among the various materials exploited for memory property, carbon-based nanomaterials such as graphene oxide has been under intensive study due to its extraordinary structural and electrical properties. Recently, Yao et al. studied the reproducible current hysteresis in a two terminal SiO_2/SWCNT sandwich structure and proposed the charge trapping in the SiO_2/SWCNT interface as the phenomenon responsible for the memory properties [13]. Wu et al. fabricated PS/SLG/PMMA/SLG/PMMA multi-stacking layered device and studied the tristable resistive memory behaviour with a current ON/OFF ratio of 10^4. They proposed that the stepping-charging operation mechanism in the multi-stacking layer was responsible for the tristable memory behaviour [14]. Another group Sun et al. studied the ternary resistance switching memory behavior in graphene oxide embedded in polystyrene layer and found that the presence of the polysterene layer improved the memory properties of the device [15]. Presence of large hysteresis was found by Bartolomeo et al. in SiO_2/SWCNT with an operating cycle upto 10^5 [4]. Till date, researchers have obtained different kinds of memory property by varying the type of material used for device fabrication. But very rarely has it been tried to tune the memory properties by varying the amount of active material. In the present study, polymer based multi-stacked organic memory devices have been fabricated by using graphene oxide as the active material and the memory properties have been tuned by varying the concentration of graphene oxide**.**

EXPERIMENTAL PROCEDURE

Materials Used

Graphite flakes (Merck), sodium nitrate ($NaNO_3$) (Merck), potassium permanganate ($KMnO_4$) (Merck), sulphuric acid (H_2SO_4) (Merck), hydrogen peroxide (H_2O_2) (Merck), polymethylmetacrylate (PMMA) (Sigma Aldrich, average molecular weight (M_w): 120,000), dimethyl formamide (DMF) (Merck).

Material Synthesis and Device Fabrication

The synthesis of GOs was done by Hummer's method. Briefly, a solution of graphite flakes and $NaNO_3$ in H_2SO_4 was prepared followed by slow addition of $KMnO_4$ to it. Then the solution was heated at 35 ^{o}C before the addition of DI water. Then the solution was heated again at 96 ^{o}C followed by addition of more DI water to it. Finally H_2O_2 was added resulting in a yellowish solution. The solution was then washed with 10% HCl and DI water for several times and was then kept in a hot air oven to dry. For device fabrication, solution of PMMA (100 mg) in DMF (3 ml) was spin-coated onto ITO at 9000 rpm for 60s. Next different concentrations of graphene oxide (0.1 mg, 0.2 mg, 0.3 mg, 0.4 mg and 0.5 mg) were spin-coated onto the PMMA layer at 1000 rpm for 60 s. Then a final layer of PMMA was spin-coated on the deposited graphene oxide layer using the same concentration and deposition parameters as before. The top electrode of aluminium was deposited by using a shadow mask method in a thermal evaporation technique. A schematic diagram of the fabricated device is shown in the Fig. 1.

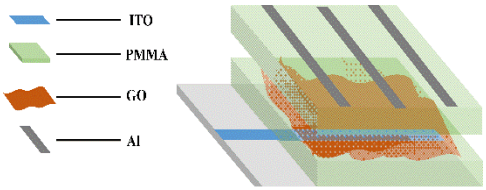

FIGURE 1. Schematic diagram of ITO/PMMA/GOs/PMMA/Al device

The fabricated devices were assigned different names corresponding to different concentrations of graphene oxide as shown in Table 1 below:

TABLE 1. List of fabricated devices

Concentration of graphene oxide	Device name
0.1 mg	D_1
0.2 mg	D_2
0.3 mg	D_3
0.4 mg	D_4

RESULTS AND DISCUSSIONS

Fig. 2(a) shows the FTIR spectra of GOs. From the spectra, the peaks at higher wavenumbers ~ 3000 – 3700 cm^{-1} can be attributed to the stretching vibrations of the hydroxyl (-OH) groups and the remanent water present in the graphene oxide sheets [16]. The presence of these hydrophilic oxygen containing functional groups are responsible for the easily dispersible nature of graphene oxide in almost any solvent. Another peak at 1280 cm^{-1} was obtained which may be due to the stretching mode of C-O-C functional groups present in the basal plane of graphene oxide [17]. The peak at 1528 cm^{-1} may be attributed to the skeletal vibrations of the aromatic rings [18]. Also the presence

of stretching vibrations of the edge bounded carbonyl groups in the synthesized graphene oxide is confirmed from the peak obtained at 1726 cm^{-1} [19]. Other functional groups include C-O (1040 cm^{-1}) [20] and C-H (2928 cm^{-1}) [21].

Fig. 2(b) shows the XRD spectra of the synthesized GOs. It was performed by using Cu Kα radiation with λ=1.54 Å in a 2Θ range of 5^{O}-60^{O}. From the figure, it can be seen that graphene oxide has a hexagonal structure. A sharp peak was obtained at 2Θ = 9.52^{O} corresponding to reflection from (002) plane of graphene oxide [22]. The interplanar spacing corresponding to the most intense peak was calculated using Bragg's Law,and was found to be about 9.28 Å. Another less intense peak at 2Θ = $19.32^{O}$was obtained which may be induced by the disordered components generated during the synthesis of graphene oxide from graphite precursor [23]. A third least intense peak was obtained at 42.42^{O} which is due to reflection from (100) plane of rGO [24].

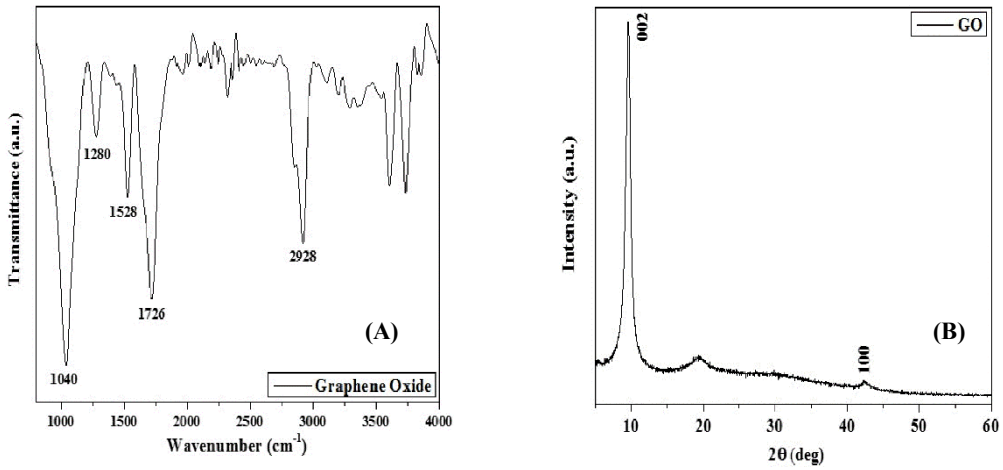

FIGURE. 2 (A) FTIR spectra and (B) XRD spectra of graphene oxide (GOs)

Current-voltage (J-V) characteristics of all the fabricated devices were studied at room temperature and is shown in the Fig. 3. During the measurement, the ITO bottom electrode was given the bias whereas the Al top electrode was grounded. From the figure it can be seen that all the devices exhibited electrical hysteresis when supplied with a sweeping voltage of -4V - +4V or more. Also the measurements were repeated for 10 cycles and it was seen that each device repeatedly exhibited the electrical hysteresis for all the cycles thereby confirming its stability with repeatable nature.

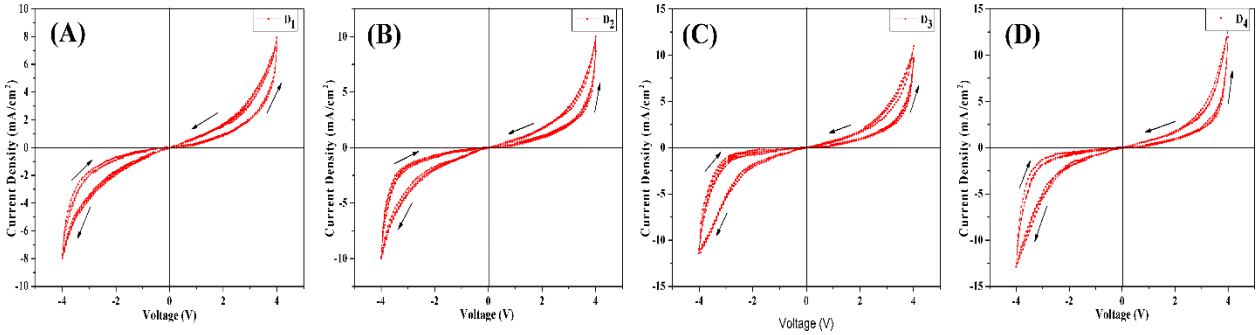

FIGURE. 3J-V characteristics of device (A) D_1(B) D_2 (C) D_3 (D) D_4

The variation of hysteresis area with the increase in concentration of graphene oxide is shown in Fig 4. From the figure it can be seen that with the increase in concentration of graphene oxide, the area under the hysteresis curve increases. This may be because at lower concentrations, the distance between the graphene oxide sheets is greater thereby causing a break to the electron flow. This results in lower current value. But with increase in concentration, the sheets of graphene oxide come together thereby forming a complete structure for the electrons to flow. As a result, the current increases leading to the overall increase in the hysteresis area.

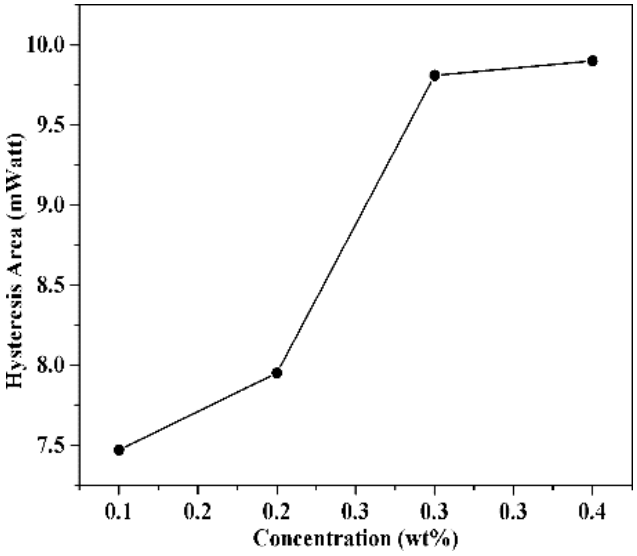

FIGURE. 4. Variation of hysteresis area with change in concentration of GOs

CONCLUSION

In summary, memory properties of multi-stacked devices based on graphene oxide were studied for probable future memory application in devices such as flash memories. In the process, graphene oxide was successfully synthesized through Hummer's method. The synthesized graphene oxide had an inter-planar spacing of about 9.28 Å and the planes preferably orienting along the (002) direction.All the fabricated devices exhibited electrical hysteresis on being supplied with an external voltage, thereby confirming the presence of memory properties. Also the area under the hysteresis curve was found to increase with increasing the concentration of graphene oxide.

REFERENCES

1. L. Zhou, J. Mao, Y. Ren, S. T. Han, V. A. L. Roy and Y. Zhou, Small,**1703126**, 1-27 (2018).
2. S. K. Pradhan, B. Xiao, S. Mishra, A. Killam and A. K. Pradhan, Scientific Reports, **6**(2016).
3. C. Tan, Z. Liu, W. Huang and H. Zhang, Chem.Soc.Rev., **44**, 2615-2628 (2015).
4. A.Di Bartolomeo, A. K. Boyd, Y. Yang and P. Barbara, Nanoscale Res Lett,**5**, 1852–1855 (2010).
5. G.Khurana, P. Misra, N. Kumar and R. S. Katiyar, J. Phys. Chem. C, **118**, 21357-21364 (2014).
6. P. Mondal, H. Mullick, T. Lavanya, A. Dhar, S. K. Ray and S. K. Lahiri, Journal of Applied Physics, **102**, 064305 (2007).
7. D. Ielmini, Semicond. Sci. Technol., **31**, 063002 (2016).
8. T. W. Kim, Y. Yang, F. Li and W. L. Kwan, NPG Asia Materials, 4 (2012).
9. B. X. D. Zhuang, Y. Chen, G. Liu, P. P. Li, C. X. Zhu, E. T. Kang, K. G.Neoh, B. Zhang, J. H. Zhu and Y. X. Li, Adv. Mater., **22**, 1731–1735 (2010).
10. H. Y.Jeong,J. Y. Lee,J. Y. Kim,T. H. Yoon,J. W. Kim,B. J. Cho,J. O. Hwang,S. O. Kim,J. E. Kim,R. S. Ruoffand S. Y. Choi, Nano Lett., **10**, 4381–4386 (2010).
11. Y. Liu, J. Zhao, L. Zhao, W. Li, H. Zhang, X. Yu and Z. Zhang, ACS Appl. Mater. Interfaces, **8** (1), 311–320 (2016).
12. Y. Sun, L. Li, D. Wen, X. Bai and G. Li,Phys. Chem. Chem. Phys., **17**, 17150-17158 (2015).
13. J. Yao,Z. Jin,L.Zhong,D. Natelson and J. M. Tour, ACS Nano.,**3**(12),4122-4126 (2009).
14. C. Wu, F. Li, and T.Guo, Appl. Phys. Lett.,**104**, 183105 (2014).
15. Y. Sun, D. Wen, X. Bai, J. Lu and C. Ai, Scientific Reports,**7**(2017).
16. G. Wang, B. Wang, J. Park, J.Yang, X. Shen and J. Yao, CARBON,**47**,68– 72 (2009).
17. Y. Si and E. T. Samulski, Nano Lett., **8** (6), 1679–1682 (2008).

18. Y. Dong, J. Shao, C. Chen, H. Li, R. Wang, Y. Chi, X. Lin and G. Chen, CARBON,**50**, 4738– 4743 (2012).
19. S.Drewniak, R.Muzyka, A.Stolarczyk, T.Pustelny, M. K. Moranskaand M.Setkiewicz, Sensors, **16**(103), (2016).
20. M.Beidaghi and C. Wang, Adv. Funct.Mater.,**22** (21),(2012).
21. S. N Kumar, S. Das, C. Bernhard and G. D.Varma, Supercond. Sci. Technol.,**26**, 095008 (2013).
22. S. S. Maktedar, S. S. Mehetre, G. Avashthi and M. Singh, UltrasonicsSonochemistry,**34**, 67–77 (2017).
23. S. Park, J. An, J. R. Potts, A. Velamakanni, S. Murali and R. S. Ruoff, Carbon, **49** (9), 3019–3023 (2011).
24. Z. Fan, K. Wang, T. Wei, J. Yan, L. Song and B. Shao,Carbon, **48** (5), 1686–1689 (2010).